

Influence of Loop Delay on LLC Converter Control Bandwidth

Nick James Kirkby, *Student Member, IEEE*, njk@asu.edu

Abstract—A 1.5 MHz LLC converter is modeled analytically and in simulation to answer the question: what is the upper limit on stable control bandwidth given the sensing, computation, and actuation delays of the TMS320F28379D SOC?

Index Terms—LLC converter, delay modeling.

I. INTRODUCTION

POWER converters such as the LLC are increasingly pushed to switching frequencies greater than 1 MHz to achieve miniaturization. At these high switching frequencies, delays due to sensing, control, and actuation may significantly reduce the closed-loop control bandwidth. This paper investigates the influence of these delays on the control bandwidth of a 1.5 MHz LLC converter.

II. SYSTEM MODEL

The system model is shown in Figure 1. It consists of a plant $G_p(s)$, a controller $G_c(s)$, and a feedback delay $G_D(s)$. The achievable control bandwidth may be limited by any of the three components in the feedback loop. The aim of this project is to determine which of $\{G_c(s), G_p(s), G_D(s)\}$ limits the control bandwidth of the LLC converter implementation described in section III-B.

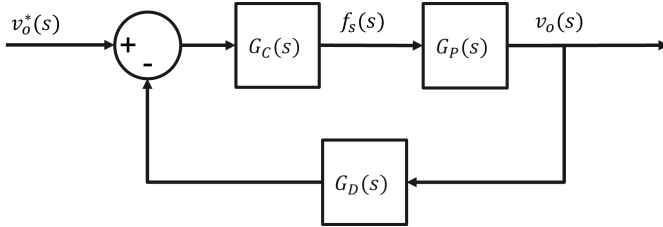


Fig. 1: Feedback system model showing the plant $G_p(s)$, the controller $G_c(s)$, and the feedback delay $G_D(s)$.

III. PLANT MODEL

Dynamic modeling of LLC converters is an active research area. The LLC converter is a nonlinear plant – its dynamics vary as a function of both the control variable f_s and also the load resistance R_L . The author selected Tian's plant transfer functions as derived in [1] as the basis for the plant model G_p .

Tian's model has more than ten parameters. To check that the model was implemented correctly, the author compared the frequency response of the analytical plant model to the frequency response of a PLECS simulation of the same converter.

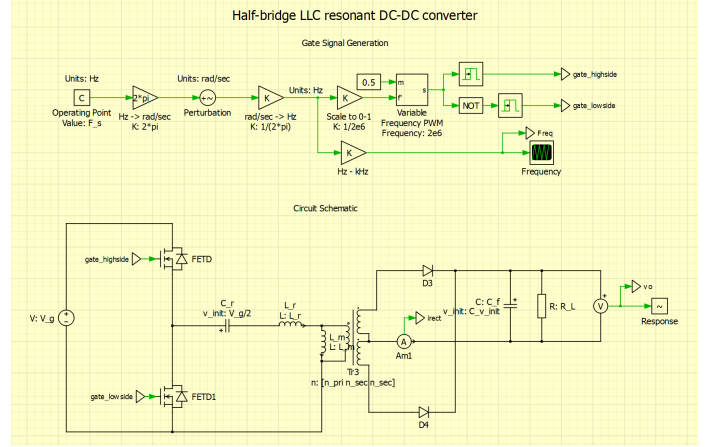


Fig. 2: LLC converter as modeled in PLECS and used to reproduce Tian's simulation results.

A. Consistency between Analytical and Simulation Models

Validation of the analytical model in simulation proved challenging as the LLC is frequency modulated and circuit simulation softwares vary greatly in their abilities to extract frequency response information from frequency-modulated switching converters. An LLC converter was modeled in PLECS based on an example implementation and multitone analysis [2] was used to extract its frequency response. The circuit is shown in Figure 2, where the small-signal perturbation is applied to the switching frequency ω_s and the output voltage v_o is the response.

Initial comparison between simulated frequency response and the analytical transfer functions created using Tian's method did not agree. The comparison is shown in Figure 3 where each model is evaluated using the converter parameters from Fig. 22 of [1]. The outputs agree closely for the $F_s = 1.4F_o$ case, but disagree for the remaining two cases.

To gain confidence in the simulated frequency response results, the PLECS multitone analysis was compared alongside Tian's SIMPLIS implementation. The comparison is shown in Figure 4 where the PLECS and SIMPLIS frequency responses are nearly identical. PLECS' multitone and SIMPLIS' periodic operating point (POP) analysis methods differ in their implementations, but both are able to extract closely matching frequency responses of the modeled converter. The parameters in the PLECS simulation were updated to match those in the SIMPLIS simulation provided to the author by Dr. Tian.

The source of the discrepancy in Figure 3 was traced back to nonideal diode models in the PLECS simulation which

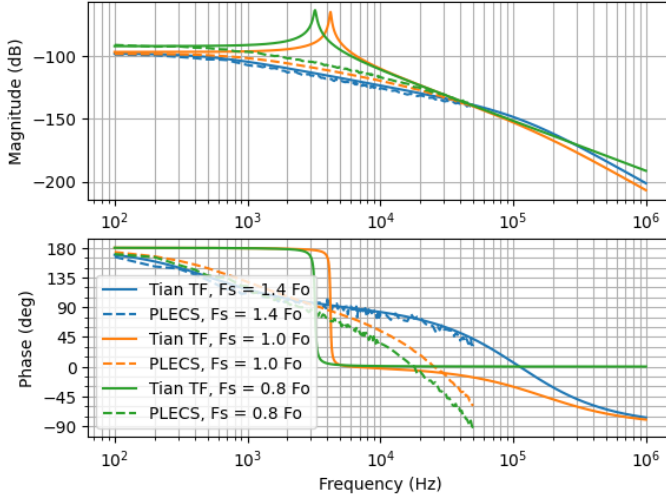


Fig. 3: Comparison of simulated frequency responses of the same converter implemented in PLECS (dashed lines) and $G_p(s)$ using Tian's method (solid lines) at $F_s = \{1.4, 1.0, 0.8\}F_o$ using converter parameters from Fig. 22 of [1]. The discrepancy was found to stem from nonideal diode models used in the PLECS simulation.

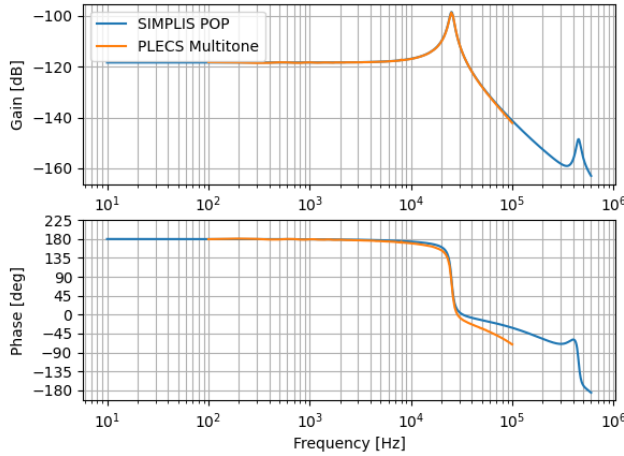


Fig. 4: Comparison of simulated frequency responses of the same converter implemented in PLECS and SIMPLIS circuit simulators.

the author adapted from a PLECS example. The second-order resonant peak in visible in the $F_s = 1.0F_o$ and $F_s = 0.8F_o$ cases is very sensitive to rectifier damping, and the simulated diode losses in the PLECS example implementation were sufficient to fully damp the resonant peak predicted by the analytical model for an LLC converter with a lossless rectifier. With the discrepancy understood, the 1.5 MHz LLC converter was modeled next.

B. Modeling the 1.5 MHz LLC Converter

The parameters in Table I were used to model the 1.5 MHz LLC converter in the remainder of this paper. This converter

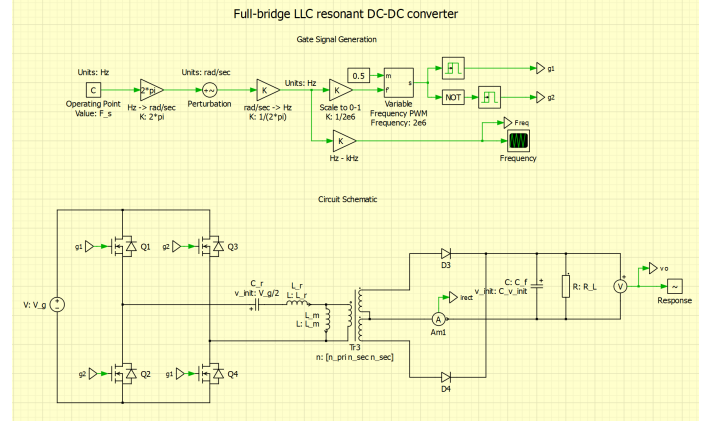


Fig. 5: LLC converter with full-bridge inverter.

is designed to deliver 1500 W at 48 V from a 270 V input. The 1500 W operating point is at $F_s = 1.0F_o$, so [1] Eqn. 14 ($F_s \geq F_o$) is used to model the plant. In this 1.5 MHz LLC converter, a full-bridge inverter is used instead of the half-bridge inverter used in [1]. Due to the voltage-doubling effect of the full bridge inverter, the control-to-output plant transfer function $G_p(s) = \frac{v_o(s)}{\omega_s(s)}$ is a factor of two larger than the half-bridge case derived by Tian [1], Eqn. 14. A schematic of the new 1.5 MHz LLC converter with full-bridge inverter is shown in Figure 5.

Parameter	Value	Description
L_r	$2 \mu H$	Resonant inductor
L_m	$10 \mu H$	Magnetizing inductor
C_r	$5.6 nF$	Resonant capacitor
C_f	$100 \mu F$	Output filter capacitor
n_{pri}	6	Transformer primary turns
n_{sec}	1	Transformer secondary turns
R_{load}	1.536Ω	Load resistance
V_o	48 V	Output voltage
V_g	270 V	Input voltage
P_o	1500 W	Output power
$F_o = \frac{1}{2\pi\sqrt{L_r C_r}}$	1.5 MHz	Resonant tank frequency

TABLE I: LLC converter parameters used in the remainder of this paper.

Finally, the analytical and simulated models were compared for the 1.5 MHz LLC using the parameters shown in Table I, and the resulting frequency responses are compared in Figure 6. The agreement of the two models is excellent, and the analytical plant model is used for compensator design in the following section.

IV. COMPENSATOR DESIGN

The open-loop plant transfer function corresponding to the LLC converter with parameters in Table I is shown in Fig. 6 and as a transfer function in (1).

$$G_p = \frac{v_o(s)}{\omega_s(s)} = \frac{-1.401 \times 10^{12}}{9.959 \times 10^6 s^2 + 7.23 \times 10^{10} s + 7.2 \times 10^{17}} \quad (1)$$

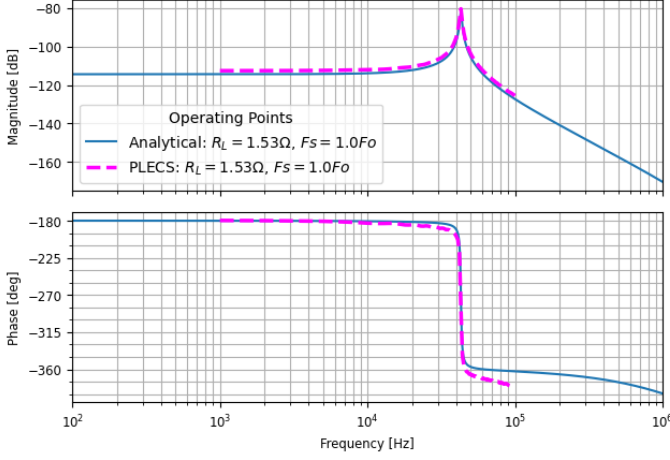


Fig. 6: Cross-validation of plant frequency responses of $G_p(s)$ based on [1] and PLECS simulation for a full-bridge LLC converter using the parameters given in Table I.

The plant transfer function (1) contains a pole pair at the resonant frequency of the output capacitance and the effective tank inductance.

The controller G_c was designed using the k-factor method [3] as taught by Dr. Raja Ayannar [4], [5], with some minor modifications. The controller design steps are as follows:

- 1) Determine the phase of the plant, ϕ_{sys} at ω_c from analytical small signal model (1).
- 2) Calculate phase boost ϕ_{boost} required, using $\phi_{boost} = PM_{desired} - \phi_{sys} - 90^\circ$.
- 3) Calculate k , ω_z , and ω_p as follows: $k = \tan(\frac{\phi_{boost}}{2})$, $\omega_z = \frac{\omega_c}{k}$, and $\omega_p = k\omega_c$.
- 4) Calculate K_c , $K_c = \frac{\omega_c}{k|G_p(j\omega_c)|}$.

The sign of the plant transfer function G_p is negative, so 180° was added to ϕ_{sys} to compensate for its negative sign. The form of the type-II k-factor controller is

$$G_c = \frac{K_c}{s} \frac{1 + \frac{s}{\omega_z}}{1 + \frac{s}{\omega_p}} \quad (2)$$

The forward-path transfer function $G_c G_p$ is the product of (2) and (1).

The phase margin $PM_{desired}$ and the crossover frequency ω_c were swept over the ranges $\{60, 90\}^\circ$ and $\{300, 5000\}Hz$ respectively and the closed loop step response and gain margin were observed. Fig. 7 shows the open-loop transfer function $G_c G_p$ for a type-II k-factor controller with $PM_{desired} = 85^\circ$ and $f_c = 1000$ Hz. The gain margin is more than 6 dB with the crossover frequency at 1000 Hz. Further increasing the crossover frequency reduces the gain margin unacceptably.

The step response of three controller variants is shown in Fig. 8. The instability due to decreasing gain margin is visible in the third case $f_c = 5000$ Hz. The best closed loop response was found at $PM_{desired} = 85^\circ$ and $f_c = 1000$ Hz, ($\omega_c = 6283 \frac{rad}{s}$).

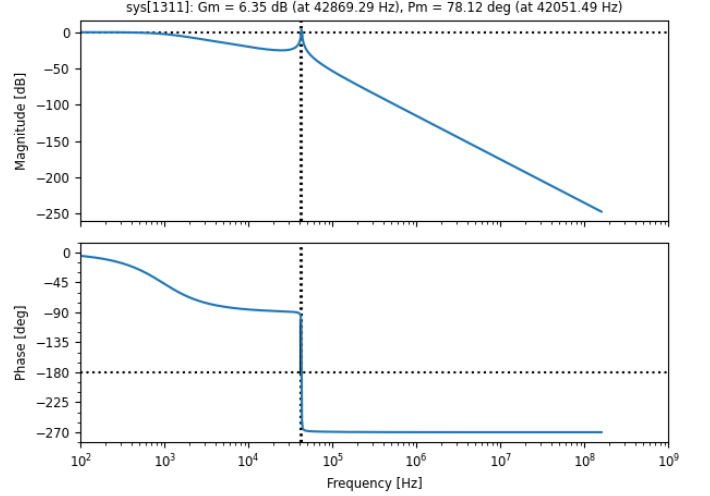


Fig. 7: $G_c G_p$ where G_c is a type-II k-factor controller with $PM_{desired} = 85^\circ$ and $f_c = 1000$ Hz.

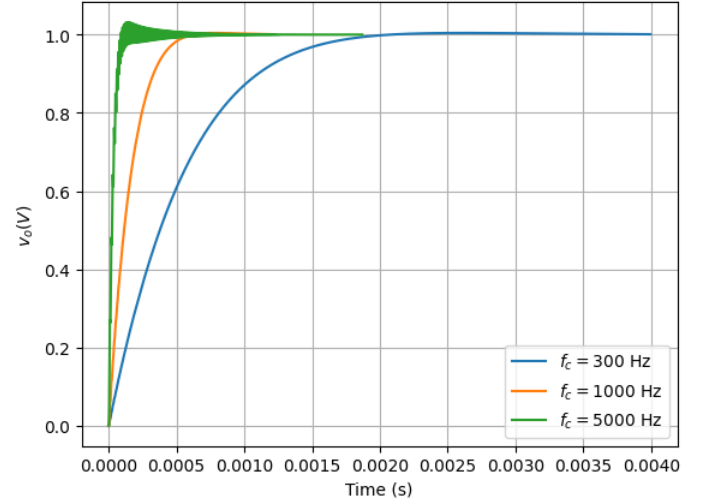


Fig. 8: Closed-loop step response for three crossover frequency values f_c .

Finally, the closed-loop frequency responses of the analytical model and the PLECS simulation were compared. The results are shown in Figure 9.

V. DELAY MODELING

The original aim of this project was to find which of $\{G_c(s), G_p(s), G_D(s)\}$ limits the control bandwidth of the LLC converter. Section IV showed that the plant $G_p(s)$ limits the control bandwidth to approximately 1 kHz due to the lightly-damped plant double pole at approximately 40 kHz. As the controller bandwidth is increased beyond 1 kHz, proximity to the double plant pole at 40 kHz results in a diminishing gain margin and closed-loop stability is compromised.

Practically speaking, a 1 kHz bandwidth controller is trivial to implement on the TMS320F28379D SOC, and further analysis of G_D is not necessary. However, the author has included a brief analysis of the delay model for completeness.

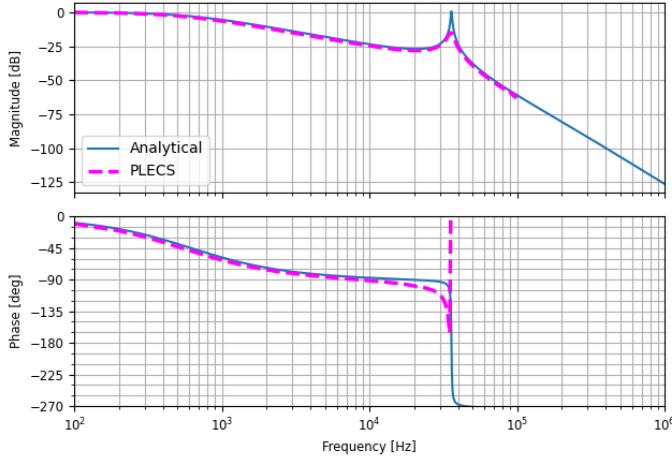


Fig. 9: Comparison of $G_{cl} = \frac{G_c G_p}{1 + G_c G_p}$ for the analytical model (solid line) and PLECS simulation (dashed line).

Also, an alternate 1.5 MHz LLC design in which the size of the filter capacitor C_f is decreased in order to push the 40 kHz plant double pole to a higher frequency is of interest to the author. A sufficient decrease in filter capacitance C_f will eventually result in the control bandwidth being limited by controller delays G_D instead of plant dynamics G_p .

A. Analytical Delay Model

Using chapter 6.8 of [6], the effects of time delays in the controller are modeled using a Pade approximation (3).

$$\angle G_D = -\omega T_d \quad (3)$$

where T_d is the delay time, ω is the frequency in $\frac{rad}{s}$, and $\angle G_D$ is the phase delay in rad .

For an embedded control application, sensing, computation and actuation are designed to run at a fixed frequency with deterministic execution time. Fig. 10 shows the phase delay contributed for four candidate loop periods of $T = \{1, 2, 10, 20\} \mu s$. A phase delay of more than 10° is considered undesirable. It can be seen from Figure 10 that even the slowest considered loop period of $20 \mu s$ does not contribute significant phase delay 1 kHz.

For control bandwidths exceeding 10 kHz, the phase delay contribution will become significant. This is the subject of future analysis.

VI. CONCLUSION

The analytical transfer functions of the LLC converter provided in [1] were validated against a PLECS simulation. A 1.5 MHz LLC was modeled and its plant transfer function used to design a type-II k-factor controller. It was found that the control bandwidth is limited by the plant double pole at approximately 40 kHz, and that delays due to sensing, computation, and actuation do not limit the control bandwidth of the 1.5 MHz LLC converter studied here.

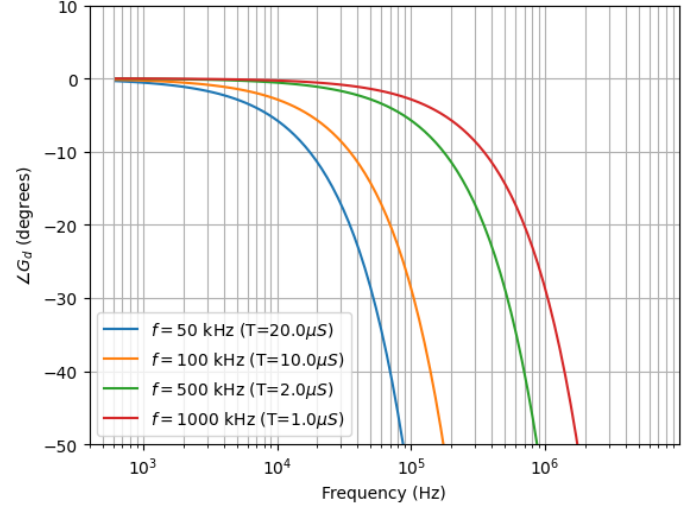


Fig. 10: Approximation of delay angle contribution $\angle G_d$ versus frequency for four loop frequencies calculated using (3).

ACKNOWLEDGMENTS

Dr. Shuilin Tian provided crucial support in reproducing his results. Dr. Jennie Si gave valuable feedback and guidance during this project.

REFERENCES

- [1] S. Tian, F. C. Lee, and Q. Li, "Equivalent Circuit Modeling of LLC Resonant Converter," *IEEE Transactions on Power Electronics*, vol. 35, no. 8, pp. 8833–8845, Aug. 2020, conference Name: IEEE Transactions on Power Electronics. [Online]. Available: <https://ieeexplore.ieee.org/document/8962014/?arnumber=8962014>
- [2] "Analysis Tools in PLECS Standalone," 2022. [Online]. Available: https://www.plexim.com/sites/default/files/tutorials_categorized/plecs/analysis_tools.pdf
- [3] H. D. Venable, "The K Factor: A New Mathematical Tool for Stability Analysis and Synthesis," San Diego, CA, 1983, pp. H1–1 to H1–12. [Online]. Available: <https://www.venableinstruments.com/hubfs/The%20K%20Factor%20a%20New%20Mathematical%20Tool%20for%20Stability%20Analysis.pdf>
- [4] R. Ayannar, "k-factor control design method: part 1 - YouTube," Jul. 2014. [Online]. Available: <https://www.youtube.com/embed/ExFV-CPvmU>
- [5] —, "k factor control design method for dc dc part2 - YouTube," Jul. 2014. [Online]. Available: <https://www.youtube.com/embed/RmREot5DUtk>
- [6] G. F. Franklin, J. D. Powell, and A. Emami-Naeini, *Feedback control of dynamic systems*, eighth edition ed. Ny, NY: Pearson, 2019.